

# Status of the hyperon-nucleon interaction in chiral effective field theory

Johann Haidenbauer<sup>1,\*</sup> and Ulf-G. Meißner<sup>2,1,\*\*</sup>

<sup>1</sup>Institute for Advanced Simulation, Institut für Kernphysik and Jülich Center for Hadron Physics, Forschungszentrum Jülich, D-52425 Jülich, Germany

<sup>2</sup>Helmholtz-Institut für Strahlen- und Kernphysik and Bethe Center for Theoretical Physics, Universität Bonn, D-53115 Bonn, Germany

**Abstract.** The Jülich-Bonn group aims at an extensive study of the baryon-baryon ( $BB$ ) interaction involving strange baryons ( $\Lambda$ ,  $\Sigma$ ,  $\Xi$ ) within SU(3) chiral effective field theory. An overview of achievements and new developments over the past few years is provided. The topics covered are: 1) Derivation of the leading charge-symmetry breaking (CSB) interaction for the  $\Lambda N$  system and its application in a study of CSB effects in  $A=4$   $\Lambda$ -hypernuclei. 2) Updated results for the  $\Xi N$  interaction at NLO and predictions for  $\Xi^- p$  correlation functions. 3) Extension of the  $\Lambda N$ - $\Sigma N$  interaction to next-to-next-to-leading order.

## 1 Introduction

The Jülich-Bonn group explores the baryon-baryon ( $BB$ ) interaction involving hyperons within SU(3) chiral effective field theory (EFT). In this approach a potential is established via an expansion in terms of small momenta, subject to an appropriate power counting, so that the results can be improved systematically by going to higher orders, while at the same time theoretical uncertainties can be estimated [1, 2]. Furthermore, two- and three-baryon forces can be constructed in a consistent way. The resulting interaction potentials can be readily employed in standard two- and few-body calculations. They consist of contributions from an increasing number of pseudoscalar-meson exchanges, determined by the underlying chiral symmetry, and of contact terms which encode the unresolved short-distance dynamics and whose strengths are parameterized by a priori unknown low-energy constants (LECs).

The studies, performed so far up to next-to-leading order (NLO) in the chiral expansion, have shown that for the strangeness  $S = -1$  ( $\Lambda N$ ,  $\Sigma N$ ) [3, 4] and  $S = -2$  ( $\Lambda\Lambda$ ,  $\Xi N$ ) [5, 6] sectors a consistent and satisfactory description of the available scattering data and other experimental constraints can be achieved within the assumption of (broken) SU(3) flavor symmetry. Applications of the resulting potentials in bound-state calculations for light hypernuclei [4, 7–10] led to results close to the empirical values. In addition, the exploration of neutron-star properties with the strangeness  $S = -1$  interaction indicate the potential to resolve the so-called hyperon puzzle [11], when combined with consistently derived  $\Lambda NN$  and  $\Sigma NN$  three-body forces [12, 13]. Finally, the  $BB$  potentials have been successfully tested

---

\*e-mail: j.haidenbauer@fz-juelich.de

\*\*e-mail: meissner@hiskp.uni-bonn.de

in the analysis of two-particle momentum correlation functions involving strange baryons [14–16].

In this contribution we present some highlights from recent investigations. In Sect. 2 preliminary results of an extension of the  $\Lambda N$ - $\Sigma N$  interaction up to next-to-next-to leading order (N<sup>2</sup>LO) [17] are reported. In Sect. 3 a calculation of charge-symmetry breaking (CSB) of the separation energies of the  $A=4$   $\Lambda$ -hypernuclei  ${}^4_{\Lambda}\text{He}$  and  ${}^4_{\Lambda}\text{H}$  is reviewed [18]. Finally, in Sect. 4 selected results involving the  $\Xi N$  interaction [6] are summarized. Specifically, predictions for the  $\Xi^- p$  momentum correlation function are provided [15].

## 2 $\Lambda N$ - $\Sigma N$ interaction at next-to-next-to-leading order

While the description of the  $NN$  interaction within chiral EFT has been already pushed up to the fifth order [19, 20], corresponding applications of that framework to the  $YN$  interaction are lagging far behind. Here, NLO is presently the state of the art [3–6]. That status is primarily a consequence of the unsatisfactory situation with regard to the data base where practically only cross sections are available and primarily for energies near the thresholds. In particular, differential observables that would allow to fix the LECs in  $P$ - and/or higher partial waves, which arise in the chiral expansion when going to higher order, are rather scarce and of low statistics. Only within the last few years the overall circumstances became more promising, thanks to experiments performed by the E40 Collaboration at the J-PARC facility. That collaboration has already published differential cross sections for the  $\Sigma^+ p$  and  $\Sigma^- p$  channels for momenta from 440 MeV/c to 850 MeV/c [21–23] and corresponding measurements for  $\Lambda p$  are in the stage of preparation, including possibly even spin-dependent observables.

This development was one of the reasons to extend our study of the  $\Lambda N$ - $\Sigma N$  interaction to the next order. However, there are also several theoretical aspects which make an extension to N<sup>2</sup>LO rather interesting. One of them is that in the Weinberg counting three-baryon forces emerge at this order. Calculations of the four-body systems  ${}^4_{\Lambda}\text{H}$  and  ${}^4_{\Lambda}\text{He}$  for the NLO13 [3] and NLO19 [4] potentials based on the Faddeev-Yakubovsky equations indicate that the experimental separation energies are underestimated [4]. Thus, there is obviously a need for including  $\Lambda NN$  and possibly also  $\Sigma NN$  three-body forces. Another appealing factor is (in view of the mentioned scarcity of data) that no new LECs appear at this order. At the same time pertinent results for  $NN$  scattering indicate that there is some improvement in the energy dependence of the  $S$ -waves and, specifically, in several  $P$ -waves once the contributions involving the sub-leading  $\pi N$  vertices that enter at N<sup>2</sup>LO are taken into account. Certainly, no major improvement can be expected with regard to the residual regulator dependence [24]. In general, a substantial reduction of regulator artifacts can be only achieved by going to high order where then the larger number of LECs allows one to absorb the regulator dependence more efficiently. Since our calculation is at low order it is advantageous to keep such artifacts as small as possible. For that purpose a novel regularization scheme proposed and applied in Ref. [19] seems to be rather promising. Here a local regulator is applied to the pion-exchange contributions and only the contact terms, being non-local by themselves, are regularized with a non-local function. (In earlier works the latter has been applied to the whole potential [3, 4, 25].) Accordingly, the resulting interactions were called “Semilocal momentum-space regularized (SMS) chiral  $NN$  potentials” [19]. A local regulator for pion-exchange contributions leads to a reduction of the distortion in the long-range part of the interaction and, thereby, facilitates a more rapid convergence with increasing chiral order. Of course, this effect cannot be directly quantified in case of  $\Lambda N$  and  $\Sigma N$  because of the lack of corresponding empirical information. Nonetheless, given that we want to compare with the new J-PARC data at momenta around 500 MeV/c a reduction of regulator artifacts is definitely desirable.

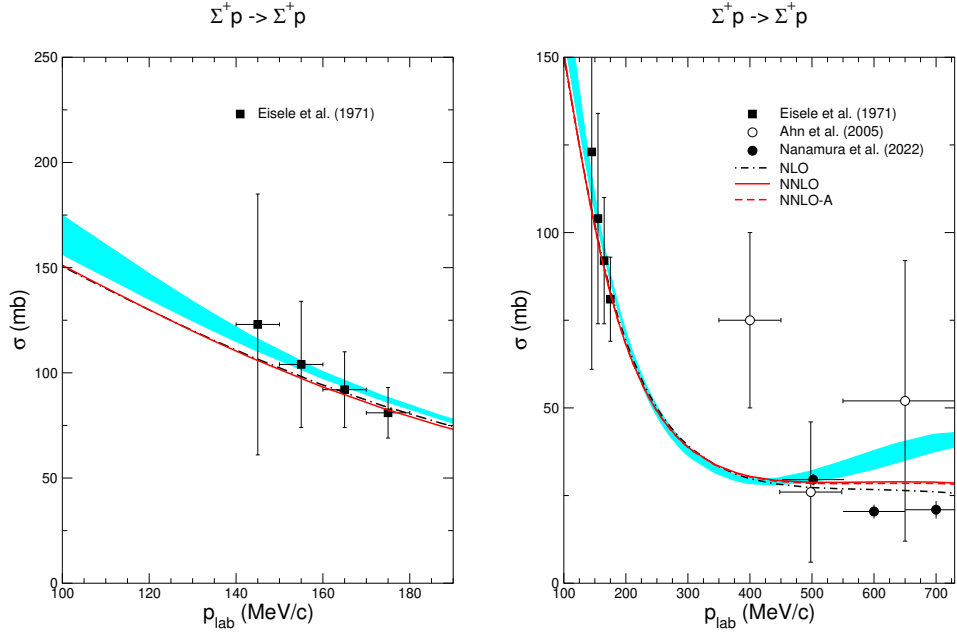


**Figure 1.** Cross section for  $\Sigma^+ p$  scattering as a function of  $p_{lab}$ . Results are shown for the SMS NLO (dash-dotted) and  $N^2$ LO (solid)  $YN$  potentials. The dashed line corresponds to an alternative fit at  $N^2$ LO, see text. The cyan band is the result for NLO19 [4]. Data are from the E40 Collaboration [23] and from Refs. [28, 29].

The extension of our  $YN$  interaction up to  $N^2$ LO builds on the SMS scheme proposed in Ref. [19]. Details of the formalism will be reported elsewhere [17]. However, for illustration we show how the non-local exponential regulator employed in our  $YN$  potentials NLO13 [3] and NLO19 [4] for the meson-exchange part is replaced by a local regularization,

$$V_P^{\text{non-local}} \propto \frac{e^{-\frac{p'^4 + p^4}{\Lambda^4}}}{\vec{q}^2 + M_P^2} \rightarrow V_P^{\text{local}} \propto \frac{e^{-\frac{\vec{q}^2 + M_P^2}{\Lambda^2}}}{\vec{q}^2 + M_P^2}. \quad (1)$$

Here  $P$  stands for  $\pi$ ,  $K$ , or  $\eta$ ,  $\vec{p}$  and  $\vec{p}'$  are the incoming and outgoing center-of-mass momenta of the baryons,  $\vec{q} = \vec{p}' - \vec{p}$  is the momentum transfer, and  $\Lambda$  is the cutoff parameter.

In the  $NN$  case, where only pion exchanges are taken into account, cutoff values in the range  $\Lambda = 350 - 550$  MeV were considered where  $\Lambda = 450$  MeV yielded the best result [19]. The choice of the cutoff mass for the  $YN$  interaction is more delicate, because we want to keep the underlying approximate SU(3) flavor symmetry as well as the explicit SU(3) breaking in the long-range part of the potential due to the mass splitting between the pseudoscalar mesons  $\pi$ ,  $K$ , and  $\eta$ . Since the kaon mass is around 495 MeV it seems advisable to use cutoff masses that are at least 500 MeV, in order to capture the pertinent physics. On the other hand, large values, say above 650 MeV, are questionable because, like in  $NN$ , we want to avoid spurious bound states. These considerations suggest that two-meson exchange contributions involving a  $K$  and/or  $\eta$  ( $\pi K$ ,  $KK$ , etc.) should and can no longer be included explicitly but have to be absorbed into the contact terms. Thus, contrary to our earlier work [3, 4] we allow and expect some SU(3) breaking between the LECs in the  $\Lambda N$  and  $\Sigma N$  systems.

In the following we present preliminary results for the cutoff value of 550 MeV. We focus on the  $\Sigma N$  channels where new data from J-PARC have become available. We start

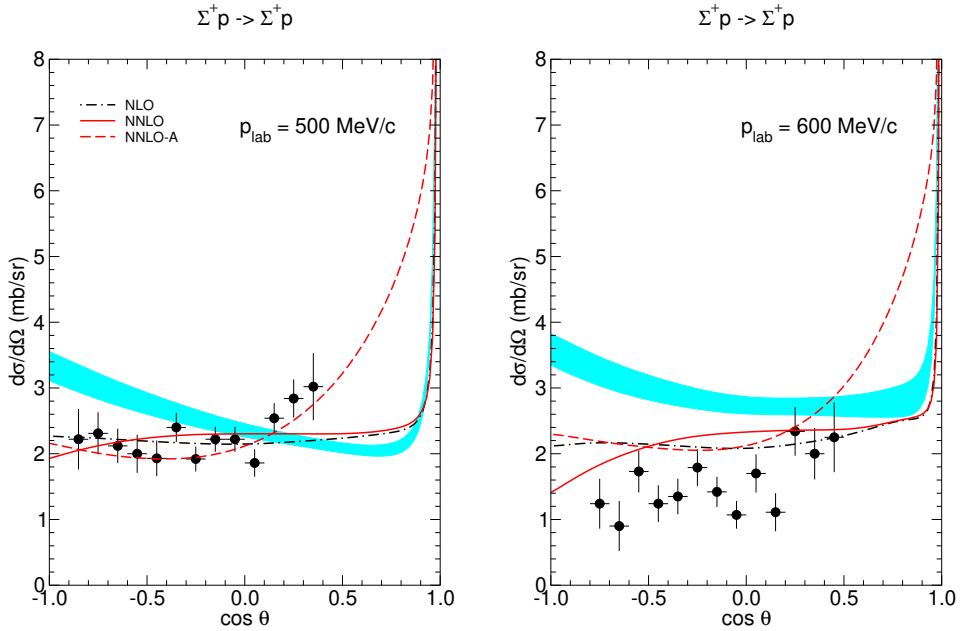


**Figure 2.** Differential cross section for  $\Sigma^+p$ . Same description of curves as in Fig. 1. Data are from Nanamura et al. [23] (momentum regions 440-550 MeV/c and 550-650 MeV/c).

the discussion with  $\Sigma^+p$  scattering which is of particular interest for theory. Since the total isospin is  $I = 3/2$  there is no coupling to the  $\Lambda N$  channel which simplifies the dynamics. Moreover, SU(3) symmetry provides strong constraints on several amplitudes. Specifically, space-spin antisymmetric partial waves ( $^1S_0, ^3P_{0,1,2}, \dots$ ) belong all to the {27} irrep. of SU(3) symmetry [3, 4] and, thus, the corresponding interactions would be identical to those in the  $NN$  system provided that SU(3) symmetry is exactly fulfilled. While we know that there is a sizable SU(3) breaking in case of the  $^1S_0$  partial wave [26], the amplitudes in the  $P$ - and higher partial waves could be much closer to those found for  $NN$  scattering.

In fitting to the  $YN$  data we proceed as before [3, 4], i.e. we consider only the set of 36 data for  $\Lambda p$ ,  $\Sigma^-p$  and  $\Sigma^+p$  scattering at low energies for determining the LECs in the  $S$  waves. SU(3) symmetry is imposed for the contact terms at the initial stage but eventually relaxed for the LO LECs, in line with the power counting where SU(3) breaking terms arise from mass insertions in the chiral Lagrangian at the NLO level [27]. Anyway, as said we do expect some SU(3) breaking in the contacts terms in view of the fact that two-meson exchange contributions from  $\pi K$ ,  $\pi\eta$ , etc. are not explicitly included. The achieved  $\chi^2$  is comparable to the one found for our NLO interactions [3, 4], and typically around 16 for the 36 data points. The pertinent results for  $\Sigma^+p$  are presented in Fig. 1 (left) and compared with data and with the results obtained from the NLO19 potential. The latter are shown as bands, representing the cutoff dependence [4].

Once the  $S$ -wave LECs are fixed, a fit to the differential cross sections reported by the E40 Collaboration is performed, starting with the  $\Sigma^+p$  data for the reasons discussed above. Interestingly, in the NLO case taking over the LECs in the  $^3P_{0,1,2}$  partial waves from the corresponding  $NN$  potential by Reinert et al. [19], in accordance with SU(3) symmetry, (and assuming the LEC in the  $^1P_1$  to be zero) yields already a good description of the E40 data taken in the region 440-550 MeV/c, cf. Fig. 2 (left). For the N<sup>2</sup>LO interaction all  $P$ -wave LECs are fitted to the data. Actually, here we explore two scenarios, one where the resulting

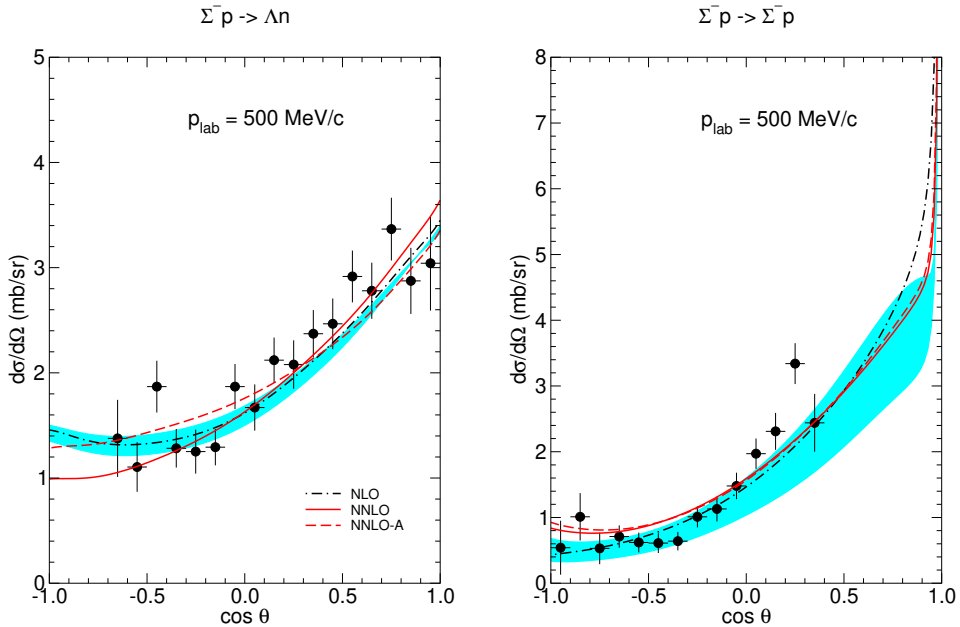


**Figure 3.** Differential cross sections for  $\Sigma^- p \rightarrow \Lambda n$  and  $\Sigma^- p \rightarrow \Sigma^- p$ . Same description of curves as in Fig. 1. Data are from the E40 Collaboration [21, 22] (momentum region 470-550 MeV/c).

angular distribution is similar to that obtained for NLO and one which produces an overall more pronounced angular dependence. The latter is clearly preferred by the available data in that momentum range. Unfortunately, the data for the next momentum region, 550-650 MeV/c, suggest an overall somewhat different angular dependence, see Fig. 2 (right), so that conclusions are difficult to draw at present. In any case the predictions by NLO19 are clearly at odds with the data.

The integrated  $\Sigma^+ p$  cross section over a larger energy range is shown in Fig. 1 (right). Note that the common angular averaging is performed here, cf. e.g. Eq. (24) in Ref. [3], for the E40 data (and accordingly for the theory results) in order to compensate for the incomplete angular coverage. Again the NLO19 potential does not reproduce the trend of the data. We believe that the rise of the cross section for larger  $p_{lab}$  could be an artifact of the employed regulator. Anyway,  $p_{lab} = 600$  MeV/c corresponds to a laboratory energy of  $T_{lab} \approx 150$  MeV so that we are certainly in a region where NLO and possibly even N<sup>2</sup>LO cannot be expected to be quantitatively reliable. Moreover, one should keep in mind that the  $\Lambda N\pi$  channel opens around that energy.

Results for the differential cross sections in the reactions  $\Sigma^- p \rightarrow \Sigma^- p$  and  $\Sigma^- p \rightarrow \Lambda n$  are presented in Fig. 3. In this case there is good agreement with the E40 data for all considered  $YN$  potentials.

### 3 Charge symmetry breaking in $A=4$ $\Lambda$ -hypernuclei

In Ref. [18] we have studied effects from CSB in the  $YN$  interaction based on the potentials NLO13 and NLO19. Specifically, we have utilized the experimentally known difference of the  $\Lambda$  separation energies in the mirror nuclei  ${}^4_{\Lambda}\text{He}$  and  ${}^4_{\Lambda}\text{H}$  to constrain the  $\Lambda$ -neutron interaction. The CSB part of the  $\Lambda N$  potential at NL $\emptyset$  (in the notation of [25]) is given by

**Table 1.**  $\Lambda p$  and  $\Lambda n$  scattering lengths (in fm) in the singlet and triplet  $S$  waves for the NLO19 potential, for cutoffs of 500-650 MeV. In addition, the resulting level splittings for the  $A = 4$  mirror nuclei  ${}^4_{\Lambda}\text{H}$  and  ${}^4_{\Lambda}\text{He}$  (in keV) are listed.

	$a_s^{\Lambda p}$	$a_s^{\Lambda n}$	$a_t^{\Lambda p}$	$a_t^{\Lambda n}$	$\Delta E(0^+)$	$\Delta E(1^+)$
NLO19(500)	-2.649	-3.202	-1.580	-1.467	249	-75
NLO19(550)	-2.640	-3.205	-1.524	-1.407	252	-72
NLO19(600)	-2.632	-3.227	-1.473	-1.362	243	-67
NLO19(650)	-2.620	-3.225	-1.464	-1.365	250	-69

[18]

$$\begin{aligned}
 V_{\Lambda N \rightarrow \Lambda N}^{CSB} = & \left[ -f_{\Lambda\Lambda\pi}^{(\Lambda-\Sigma^0)} f_{NN\pi} \frac{(\boldsymbol{\sigma}_1 \cdot \mathbf{q})(\boldsymbol{\sigma}_2 \cdot \mathbf{q})}{\mathbf{q}^2 + M_{\pi^0}^2} \right. \\
 & - f_{\Lambda\Lambda\pi}^{(\eta-\pi^0)} f_{NN\pi} (\boldsymbol{\sigma}_1 \cdot \mathbf{q})(\boldsymbol{\sigma}_2 \cdot \mathbf{q}) \left( \frac{1}{\mathbf{q}^2 + M_{\pi^0}^2} - \frac{1}{\mathbf{q}^2 + M_{\eta}^2} \right) \\
 & \left. + \frac{1}{4}(1 - \boldsymbol{\sigma}_1 \cdot \boldsymbol{\sigma}_2) C_{1S_0}^{CSB} + \frac{1}{4}(3 + \boldsymbol{\sigma}_1 \cdot \boldsymbol{\sigma}_2) C_{3S_1}^{CSB} \right] \tau_N. \quad (2)
 \end{aligned}$$

The CSB contributions arise from a non-zero  $\Lambda\Lambda\pi$  coupling constant which is estimated from  $\Lambda - \Sigma^0$  ( $f_{\Lambda\Lambda\pi}^{(\Lambda-\Sigma^0)}$ ) and  $\eta - \pi^0$  ( $f_{\Lambda\Lambda\pi}^{(\eta-\pi^0)}$ ) mixing [30], respectively, and from two contact terms,  $C_{1S_0}^{CSB}$  and  $C_{3S_1}^{CSB}$ , that represent short-ranged CSB forces. In addition, there is a small contribution due to the mass difference between  $K^\pm$  and  $K^0$  [18].  $\tau_p = 1$  and  $\tau_n = -1$ .

In order to fix the LECs  $C_{1S_0}^{CSB}$  and  $C_{3S_1}^{CSB}$  in Eq. (2) the observed CSB splittings for the  $A = 4$  hypernuclei, defined in the usual way in terms of the separation energies,

$$\Delta E(0^+) = E_{\Lambda}^{0^+}({}^4_{\Lambda}\text{He}) - E_{\Lambda}^{0^+}({}^4_{\Lambda}\text{H}), \quad \Delta E(1^+) = E_{\Lambda}^{1^+}({}^4_{\Lambda}\text{He}) - E_{\Lambda}^{1^+}({}^4_{\Lambda}\text{H}), \quad (3)$$

is considered. We aim at a reproduction of the present experimental situation, established by the recent measurements of the  ${}^4_{\Lambda}\text{H}$   $0^+$  state in Mainz [31] and the one of the  ${}^4_{\Lambda}\text{He}$   $1^+ - 0^+$  splitting at J-PARC [32], which implies  $\Delta E(0^+) = 233 \pm 92$  keV and  $\Delta E(1^+) = -83 \pm 94$  keV.

Our results for NLO19 are summarized in Table 1. One can see that the reproduction of the splittings  $\Delta E(0^+)$  and  $\Delta E(1^+)$  requires a sizable difference between the strength of the  $\Lambda p$  and  $\Lambda n$  interactions in the  $1S_0$  state. The modifications in the  $3S_1$  partial wave are much smaller and the effect goes also in the opposite direction, i.e. while for  $1S_0$  the  $\Lambda p$  interaction is found to be noticeably less attractive than  $\Lambda n$ , in case of  $3S_1$  it is slightly more attractive. In terms of the pertinent scattering lengths we predict for  $\Delta a^{CSB} = a_{\Lambda p} - a_{\Lambda n}$  a value of  $0.62 \pm 0.08$  fm for the  $1S_0$  partial wave and  $-0.10 \pm 0.02$  fm for  $3S_1$ . An investigation of CSB in  $A = 7, 8$   $\Lambda$ -hypernuclei is in preparation [38].

## 4 Aspects of the $\Xi N$ interaction

Chiral potentials up to NLO for the  $BB$  interaction in the strangeness  $S = -2$  system  $\Xi N$  have been already established by us in 2016 [5]. Thereby constraints from the  $\Lambda\Lambda$  scattering length in the  $1S_0$  state together with experimental upper bounds on the cross sections for  $\Xi N$  scattering and for the transition  $\Xi N \rightarrow \Lambda\Lambda$  have been exploited. This allowed us to fix the additional LECs that arise in the  $\{1\}$  irreducible representation of  $SU(3)$  [5]. Furthermore, the consideration of those empirical constraints necessitated to add  $SU(3)$  symmetry breaking

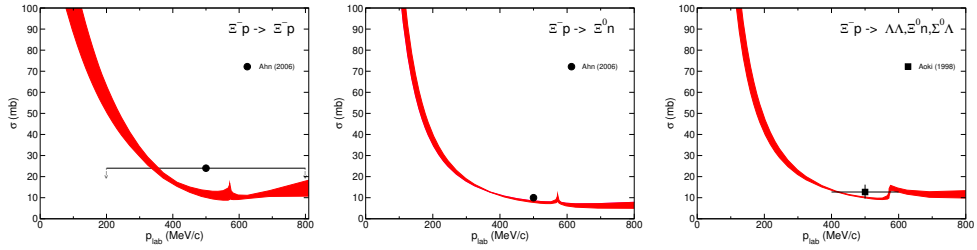


**Figure 4.** Results for the  $\Xi N$  cross sections of our NLO potential [6]. Data are from Refs. [36, 37].

contact terms in other irreps ( $\{27\}$ ,  $\{10\}$ ,  $\{10^*\}$ ,  $\{8_s\}$ ,  $\{8_a\}$ ), with regard to those determined from the  $\Lambda N$  and  $\Sigma N$  data. This is anyway expected and fully in line with the power counting of SU(3) chiral EFT, as already mentioned in Sect. 2. In 2019 a modified version has been suggested [6] which is more attractive in the  $^3S_1$  partial wave with isospin  $I = 1$ . That potential yields a moderately attractive (in-medium)  $\Xi$ -nuclear interaction [6, 33] and supports the existence of bound  $\Xi$ -hypernuclei [9], in accord with experimental evidence [34, 35]. The interactions in the  $(I = 0, 1) ^1S_0$  partial waves are the same in the two versions.

Results for the  $\Xi N$  cross sections based on the  $\Xi N$  potential from 2019 are presented in Fig. 4. An interesting and independent test for the  $\Xi N$  interaction is provided by two-particle momentum correlations. For  $\Xi^- p$ , correlation functions have been measured recently by the ALICE Collaboration in  $p$ -Pb collisions at 5.02 TeV [39] and in  $pp$  collisions at 13 TeV [40]. There are also new and still preliminary results from Au+Au collisions at 200 GeV by the STAR Collaboration [41]. In Fig. 5 we present predictions for  $C(k)$  for the  $S = -2$  interaction from 2019. The bands reflect the residual cutoff dependence [6]. Details on the evaluation of such correlation functions can be found, e.g., in Refs. [42, 43]. Clearly, the correlation functions, evaluated for the source radii  $R$  taken from the corresponding  $pp$  fits by ALICE [44] (1.43 fm for 5.02 TeV and 1.18 fm for 13 TeV), agree nicely with the measurements. For a more thorough discussion on the choice of  $R$  and of the other parameters that enter into the calculation, see [15, 43].

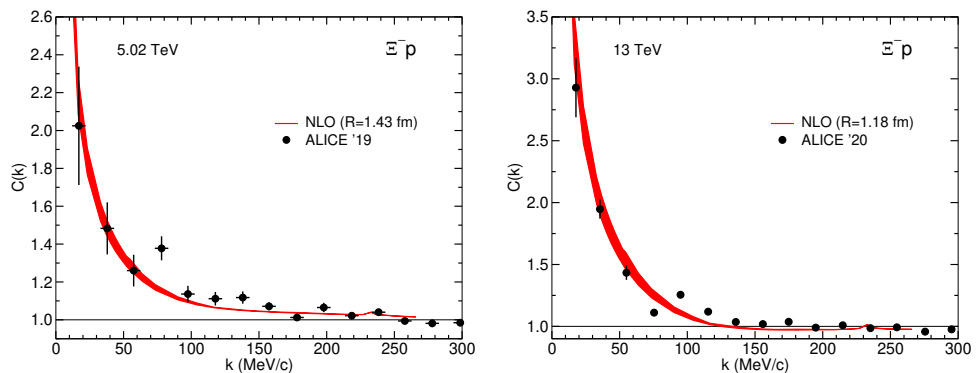


**Figure 5.** Predictions for the  $\Xi^- p$  two-particle momentum correlation function  $C(k)$  of our NLO potential [6]. Data are from the ALICE Collaboration [39, 40].

**Acknowledgements:** Work supported by the European Research Council (ERC) under the European Union’s Horizon 2020 research and innovation programme (grant no. 101018170, EXOTIC), and by the DFG and the NSFC through funds provided to the Sino-German CRC 110 “Symmetries and the Emergence of Structure in QCD” (DFG grant. no. TRR 110).

## References

- [1] E. Epelbaum, H.-W. Hammer and U.-G. Meißner, *Rev. Mod. Phys.* **81**, 1773 (2009)
- [2] R. Machleidt and D. R. Entem, *Phys. Rept.* **503**, 1 (2011)
- [3] J. Haidenbauer, S. Petschauer, N. Kaiser, U.-G. Meißner, A. Nogga and W. Weise, *Nucl. Phys. A* **915**, 24 (2013)
- [4] J. Haidenbauer, U.-G. Meißner and A. Nogga, *Eur. Phys. J. A* **56**, 91 (2020)
- [5] J. Haidenbauer, U.-G. Meißner and S. Petschauer, *Nucl. Phys. A* **954**, 273 (2016)
- [6] J. Haidenbauer and U.-G. Meißner, *Eur. Phys. J. A* **55**, 23 (2019)
- [7] H. Le, J. Haidenbauer, U.-G. Meißner and A. Nogga, *Eur. Phys. J. A* **56**, 301 (2020)
- [8] H. Le, J. Haidenbauer, U.-G. Meißner and A. Nogga, *Eur. Phys. J. A* **57**, 217 (2021)
- [9] H. Le, J. Haidenbauer, U.-G. Meißner and A. Nogga, *Eur. Phys. J. A* **57**, 339 (2021)
- [10] Hoai Le, Contribution to these proceedings, arXiv:2210.02860
- [11] D. Chatterjee and I. Vidaña, *Eur. Phys. J. A* **52**, 29 (2016)
- [12] J. Haidenbauer, U.-G. Meißner, N. Kaiser and W. Weise, *Eur. Phys. J. A* **53**, 121 (2017)
- [13] D. Gerstung, N. Kaiser and W. Weise, *Eur. Phys. J. A* **56**, 175 (2020)
- [14] S. Acharya *et al.* [ALICE], *Phys. Lett. B* **833**, 137272 (2022)
- [15] J. Haidenbauer and U.-G. Meißner, [arXiv:2201.08238 [nucl-th]]
- [16] ALICE, doi:10.1016/j.physletb.2022.137223 [arXiv:2204.10258 [nucl-ex]]
- [17] J. Haidenbauer *et al.*, in preparation
- [18] J. Haidenbauer, U.-G. Meißner and A. Nogga, *Few Body Syst.* **62**, 105 (2021)
- [19] P. Reinert, H. Krebs and E. Epelbaum, *Eur. Phys. J. A* **54**, 86 (2018)
- [20] D. R. Entem, R. Machleidt and Y. Nasyk, *Phys. Rev. C* **96**, 024004 (2017)
- [21] K. Miwa *et al.* [J-PARC E40], *Phys. Rev. C* **104**, 045204 (2021)
- [22] K. Miwa *et al.* [J-PARC E40], *Phys. Rev. Lett.* **128**, 072501 (2022)
- [23] T. Nanamura *et al.* [J-PARC E40], *Prog. Theor. Exp. Phys.* **2022**, 093D01 (2022)
- [24] E. Epelbaum, H. Krebs and U.-G. Meißner, *Eur. Phys. J. A* **51**, 53 (2015)
- [25] E. Epelbaum, W. Glöckle and U.-G. Meißner, *Nucl. Phys. A* **747**, 362 (2005)
- [26] J. Haidenbauer, U.-G. Meißner and S. Petschauer, *Eur. Phys. J. A* **51**, 17 (2015)
- [27] S. Petschauer and N. Kaiser, *Nucl. Phys. A* **916**, 1 (2013)
- [28] F. Eisele, H. Filthuth, W. Föhlich, V. Hepp and G. Zech, *Phys. Lett.* **37B**, 204 (1971)
- [29] J. K. Ahn *et al.* [KEK-PS E289], *Nucl. Phys. A* **761**, 41 (2005)
- [30] R. H. Dalitz and F. Von Hippel, *Phys. Lett.* **10**, 153 (1964)
- [31] F. Schulz *et al.* [A1 Collaboration], *Nucl. Phys. A* **954**, 149 (2016)
- [32] T. O. Yamamoto *et al.*, *Phys. Rev. Lett.* **115**, 222501 (2015)
- [33] M. Kohno, *Phys. Rev. C* **100**, 024313 (2019)
- [34] K. Nakazawa *et al.*, *Prog. Theor. Exp. Phys.* **2015**, 033D02 (2015)
- [35] M. Yoshimoto *et al.*, *PTEP* **2021**, 7 (2021)
- [36] J. K. Ahn *et al.*, *Phys. Lett. B* **633**, 214 (2006)
- [37] S. Aoki *et al.*, *Nucl. Phys. A* **644**, 365 (1998)
- [38] Hoai Le, J. Haidenbauer, U.-G. Meißner and A. Nogga, arXiv:2210.03387
- [39] S. Acharya *et al.* [ALICE], *Phys. Rev. Lett.* **123**, 112002 (2019)
- [40] S. Acharya *et al.* [ALICE], *Nature* **588**, 232 (2020)
- [41] M. Isshiki [STAR], *EPJ Web Conf.* **259**, 11015 (2022)
- [42] J. Haidenbauer, *Nucl. Phys. A* **981**, 1 (2019)
- [43] Y. Kamiya *et al.*, *Phys. Rev. C* **105**, 014915 (2022)
- [44] S. Acharya *et al.* [ALICE], *Phys. Lett. B* **797**, 134822 (2019)